

Electronic Supplementary Information for

Layered Hybrid Lead Perovskite Single Crystals: Phase Transformations and Tunable Optical Properties

Jiewu Song,^a Yangyang Dang,^{*abc} Xiao long Liu,^a and Xutang Tao^{*a}

^a State Key Laboratory of Crystal Materials & Institute of Crystal Materials, Shandong University, No. 27 Shanda South Road, Jinan, 250100, P. R. China.

^b School of Physics and Physical Engineering, Shandong Provincial Key Laboratory of Laser Polarization and Information Technology, Qufu Normal University, 273165, Qufu, P. R. China.

^c Tianjin Key Laboratory of Molecular Optoelectronic Sciences & Department of Chemistry, School of Sciences, & Collaborative Innovation Center of Chemical Science and Engineering, Tianjin University, Tianjin, 300072, P. R. China.

Corresponding Authors:

E-mail: yeung_dang@tju.edu.cn; txt@sdu.edu.cn

Experimental Section

Fig. S1 Fluorescent photo of the monoclinic PEA_2PbI_4 single crystal covered on the surface of triclinic PEA_2PbI_4 single crystal under UV-445 nm irradiation.

Fig. S2 Green emissive PEA_2PbI_4 single crystal obtained by the phase transformation processes induced by CH_3OH solvent.

Fig. S3 Red emissive PEA_2PbI_4 single crystal obtained by the phase transformation processes.

Fig. S4 Calculated and powder XRD patterns of $\text{PEA}_2\text{MA}_{n-1}\text{Pb}_n\text{I}_{3n+1}$ ($n = 1\sim 3$).

Fig. S5 Thermal properties (TGA/DSC) of $\text{PEA}_2\text{MA}_{n-1}\text{Pb}_n\text{I}_{3n+1}$ ($n = 1\sim 3$).

Fig. S6 UV-vis spectra and band gap of $\text{PEA}_2\text{MA}_{n-1}\text{Pb}_n\text{I}_{3n+1}$ ($n = 1\sim 3$).

Fig. S7 PL decay lifetime of PEA_2PbI_4 and MA: PEA_2PbI_4 single crystals under UV-445 nm irradiations and emission at 520 nm

Table. S1 Crystal data and structure refinements for $\text{PEA}_2\text{MA}_{n-1}\text{Pb}_n\text{I}_{3n+1}$ ($n = 1\sim 3$).

Experimental Section

Single-crystal X-ray diffraction and Powder X-ray diffraction studies. Single-crystal X-ray diffraction and powder X-ray diffraction measurements were depicted elsewhere.¹

UV-vis-NIR diffuse reflectance spectra measurements. UV-vis-NIR diffuse reflectance spectroscopy was carried out using a Varian Cary 5000 spectrophotometer equipped with an integrating sphere over the spectral range 200-1200 nm. The $\text{PEA}_2\text{MA}_{n-1}\text{Pb}_n\text{I}_{3n+1}$ ($n = 1\sim 3$) single crystals were dried and grinded into powders. A BaSO_4 plate was used as the standard (100% reflectance). The absorption spectrum was calculated from the reflectance spectrum using the Kubelka-Munk function: $\alpha/S = (1-R)^2/(2R)$,² where α is the absorption coefficient, S is the scattering coefficient, and R is the reflectance.

Thermogravimetric analysis Measurements. Differential scanning calorimetry (DSC) and thermogravimetric analysis (TGA) were carried out using a TGA/DSC1/1600HT analyzer (METTLER TOLEDO Instruments). The $\text{PEA}_2\text{MA}_{n-1}\text{Pb}_n\text{I}_{3n+1}$ ($n = 1\sim 3$) sample were placed in a platinum crucible, and heated at a rate of $10\text{ }^\circ\text{C min}^{-1}$ from room temperature to $800\text{ }^\circ\text{C}$ under flowing nitrogen gas.

PL spectra and PL decay time measurements. The microarea PL images were collected using a Nikon fluorescence microscope and the PL spectra of $\text{PEA}_2\text{MA}_{n-1}\text{Pb}_n\text{I}_{3n+1}$ ($n = 1\sim 3$) were gathered with a Carl Zeiss Jena LSM 780 confocal laser fluorescence microscope. The decay times of as-prepared microcrystals of $\text{PEA}_2\text{MA}_{n-1}\text{Pb}_n\text{I}_{3n+1}$ ($n = 1\sim 3$) were measured at room temperature under 445 nm wavelength irradiations.

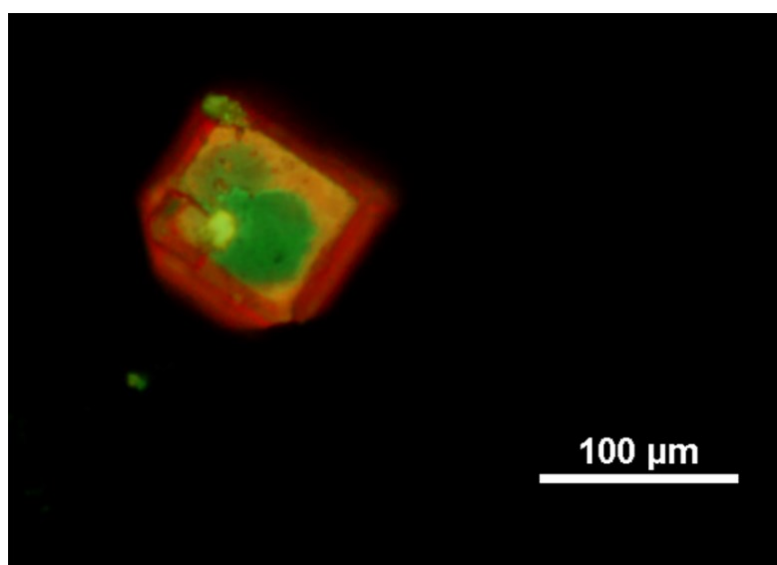


Fig. S1 Fluorescence photo of the monoclinic PEA₂PbI₄ single crystal covered on the surface of triclinic PEA₂PbI₄ single crystal under UV-445 nm irradiation.

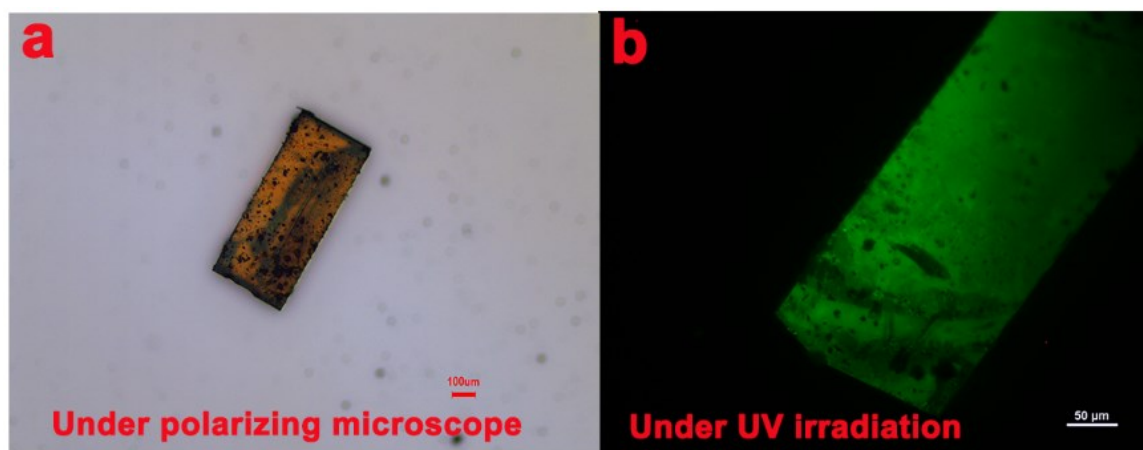


Fig. S2 Green emissive PEA₂PbI₄ single crystal obtained by the phase transformation processes induced by CH₃OH solvent. (a) PEA₂PbI₄ single crystal under polarizing microscope; (b) Green fluorescence of PEA₂PbI₄ single crystal under UV-445 nm irradiation.

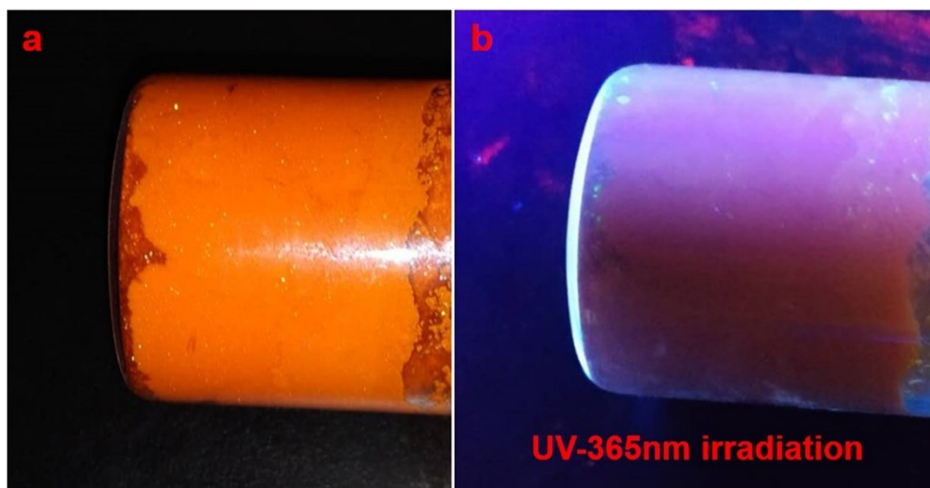


Fig. S3 Red emissive PEA_2PbI_4 single crystal obtained by the phase transformation processes. (a) PEA_2PbI_4 single crystal under ordinary light; (b) Red fluorescence of PEA_2PbI_4 single crystal under UV-365 nm irradiation.

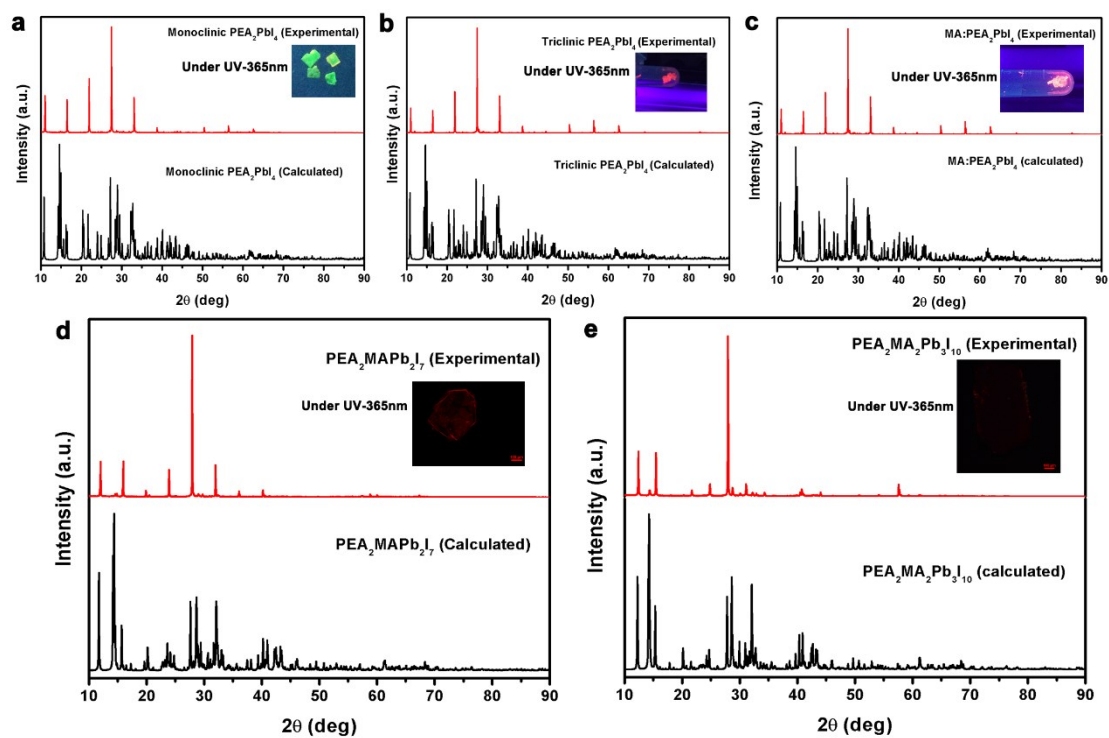


Fig. S4 Calculated and powder XRD patterns of $\text{PEA}_2\text{MA}_{n-1}\text{Pb}_n\text{I}_{3n+1}$ ($n=1\sim 3$)

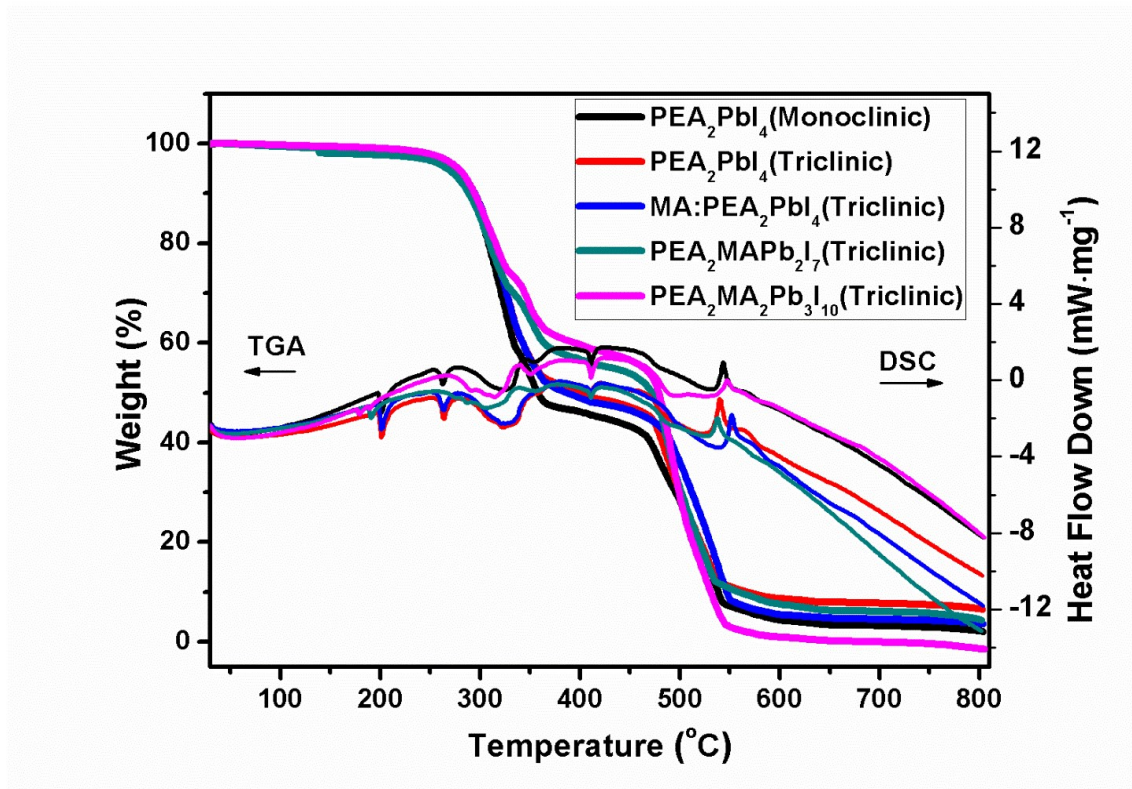


Fig. S5 Thermal properties (TGA/DSC) of $\text{PEA}_2\text{MA}_{n-1}\text{Pb}_n\text{I}_{3n+1}$ ($n = 1\sim 3$)

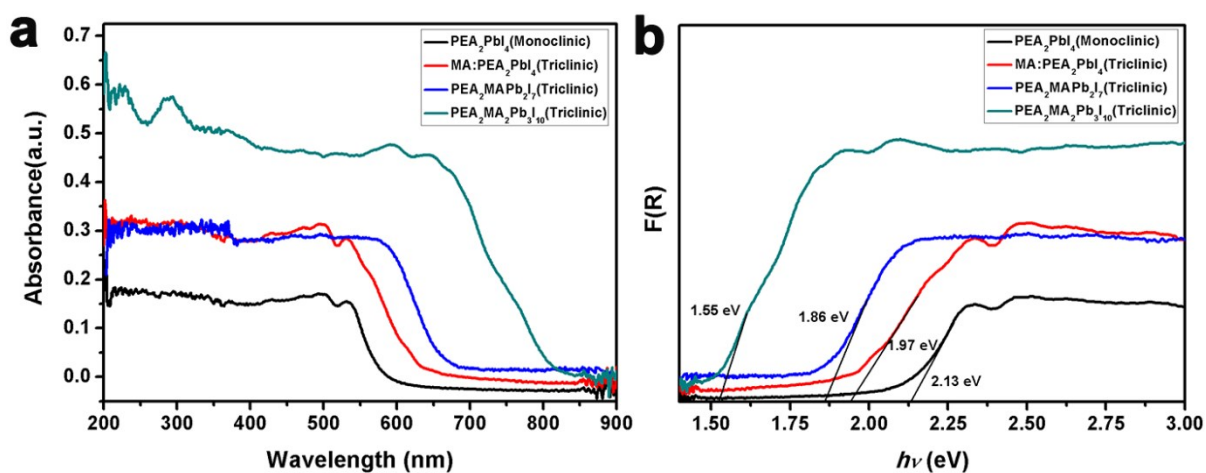


Fig. S6 UV-vis spectra and band gap of $\text{PEA}_2\text{MA}_{n-1}\text{Pb}_n\text{I}_{3n+1}$ ($n = 1\sim 3$). (a)

Tunable UV-vis spectra of $\text{PEA}_2\text{MA}_{n-1}\text{Pb}_n\text{I}_{3n+1}$ ($n = 1\sim 3$); (b) Tunable band gap of $\text{PEA}_2\text{MA}_{n-1}\text{Pb}_n\text{I}_{3n+1}$ ($n = 1\sim 3$) from 2.13 to 1.55 eV.

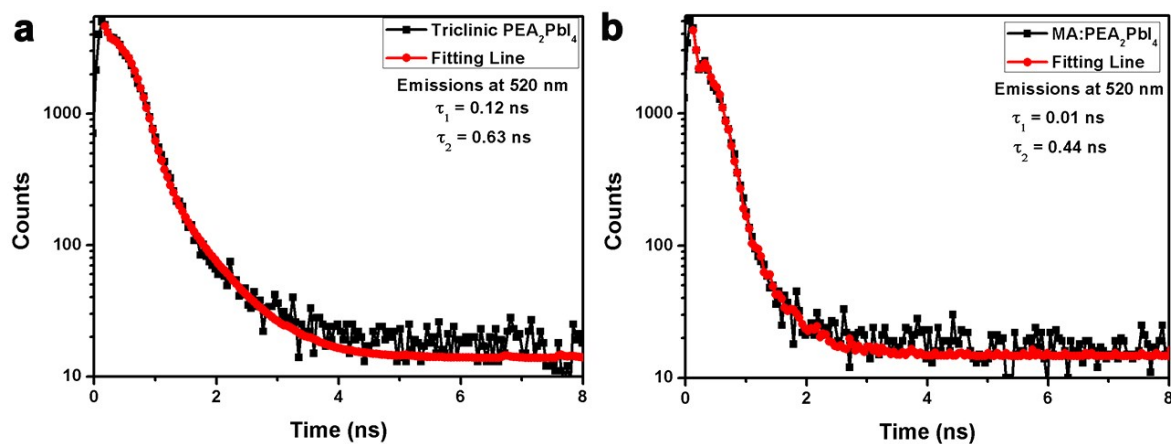


Fig. S7 PL decay lifetime of Triclinic PEA_2PbI_4 and MA: PEA_2PbI_4 under 445 nm irradiations and emission at 520 nm.

Table. S1 Crystal data and structure refinements for $\text{PEA}_2\text{MA}_{n-1}\text{Pb}_n\text{I}_{3n+1}$ ($n=1\sim 3$)

Empirical formula	$\text{C}_{16}\text{H}_{24}\text{N}_2\text{PbI}_4$		$\text{C}_{16}\text{H}_{24}\text{N}_2\text{PbI}_4$	$\text{C}_{17}\text{H}_{30}\text{N}_3\text{Pb}_2\text{I}_7$	$\text{C}_{18}\text{H}_{36}\text{N}_4\text{Pb}_3\text{I}_{10}$
Formula weight/ $\text{g}\cdot\text{mol}^{-1}$	959.16		959.16	1579.12	2199.08
Temperature/K			296(2)		
Wavelength/ \AA			0.71073		
Crystal color	Orangish	Orangish	Reddish	Brownish	Blackish
Crystal system	Monoclinic	Triclinic	Triclinic	Triclinic	Triclinic
Space group	$C2/m$ (no.12)	$P-1$ (no. 2)	$P-1$ (no. 2)	$P-1$ (no. 2)	$P-1$ (no. 2)
$a/\text{\AA}$	32.824(6)	8.7350(16)	8.7497(8)	8.8092(5)	8.8201(14)
$b/\text{\AA}$	6.1669(11)	8.7359(16)	8.7510(8)	8.8168(4)	8.8198(14)
$c/\text{\AA}$	6.2114(11)	16.673(3)	16.6830(15)	22.8196(12)	29.038(5)
$\alpha/^\circ$	90	99.694(5)	99.7643(10)	97.072(4)	93.198(2)
$\beta/^\circ$	93.205(2)	95.220(6)	95.2258(10)	93.983(4)	95.495(2)
$\gamma/^\circ$	90	90.393(5)	90.3394(10)	90.199(4)	90.123(2)
Volume/ \AA^{-3}	1255.4(4)	1248.6(4)	1253.4(2)	1754.52(15)	2245.0(6)
Crystal size (mm^3)	0.22 x 0.15 x 0.1	0.2 x 0.1 x 0.05	0.3 x 0.2 x 0.15	0.2 x 0.15 x 0.15	0.2 x 0.15 x 0.15
Z	2	2	2	2	2
Density/ $\text{g}\cdot\text{cm}^{-3}$	2.537	2.551	2.422	2.989	3.253
$\mu(\text{mm}^{-1})$	11.639	11.703	11.651	15.752	18.112
F (000)	856	856	808	1376	1896
Completeness to theta	99.1%	99.9%	99.8%	99.76%	99.8%
GOF on F^2	1.204	1.175	1.090	1.052	1.107
Absorption correction	Semi-empirical from equivalents				
Extinction coefficient	0.0142(8)	0.00005(19)	0.0033(3)	0.00075(9)	0.00106(7)
Refinement method	Full-matrix least-squares on F^2				
Data / restraints / parameters	1565/0/95	4403/0/239	4421/0/230	8472/0/164	7904/0/420
R_1, wR_2 [$I > 2\sigma(I)$]	0.0328, 0.0899	0.0525, 0.1418	0.0467, 0.1302	0.0546, 0.1443	0.0607, 0.1573
R_1, wR_2 (all data)	0.0371, 0.1051	0.0682, 0.1482	0.0514, 0.1382	0.0747, 0.1592	0.0830, 0.1734
Min/Max $\Delta\rho$ / $\text{e}\text{\AA}^{-3}$	-1.174/ 2.020	-1.600/3.513	-1.393/6.894	-1.896/2.705	-1.438/2.354
CCDC	1815922	1815926	1815923	1815925	1815924

References

- [1] Y. Dang, Y. Liu, Y. Sun, D. Yuan, X. Liu, W. Lu, G. Liu, H. Xia and X. Tao, *CrystEngComm* 2015, **17**, 665.
- [2] W. M. Wendlandt and H. G. Hecht, *Reflectance Spectroscopy*, Interscience, New York, 1966, **62**.